Progress In Electromagnetics Research, Vol. 168, 25–30, 2020

Second-Order Nonlinear Susceptibility Enhancement in Gallium Nitride Nanowires

Kangwei Wang[1], Haoliang Qian[2, *], Zhaowei Liu[1, 3], and Paul K. L. Yu[1, 3, *]

(*Invited*)

Abstract—We report the second-harmonic generation (SHG) from single GaN nanowire. The diameter of the GaN nanowire varies from 150 to 400 nm. We present a model for the SHG process in the GaN nanowire; the analysis shows quantitatively that the SHG is dominated by its surface area. The effective second order nonlinear optical susceptibility ($\chi_{eff}^{(2)}$) increases as the diameter of the GaN nanowire decreases. For 150-nm diameter GaN nanowire, $\chi_{eff}^{(2)}$ reaches 136 pm/V.

1. INTRODUCTION

Optical materials with high second-order nonlinear responses have widespread applications. For instance, second harmonic generation (SHG) is used in bio-imaging since it is less destructive to cells than the single photon process [1]. The second-order nonlinearity in electro-optic materials can also be used to make linear electro-optic modulator through the Pockels effect [2]. Among the second-order nonlinear materials, $LiNbO_3$ is the most common one to make an electro-optic (EO) modulator. It offers relatively high linear EO coefficient, r ($r_{33} = 30.9$ pm/V), and is highly transparent at 1310 nm and 1550 nm wavelengths [3]. However, $LiNbO_3$ is not compatible to most of the light emitting materials, making the integration of light source and modulator challenging. Consequently, extensive research has been focused on novel mechanisms to enhance the second-order nonlinear response based on integration friendly materials, including: strained silicon [4, 5], polymer [6], surface effect on nano-structure, metamaterials [7], and plasmonic effect [8].

Recent published papers reveal that the second order nonlinear response could be enhanced by using nanowires/nanopillars instead of bulk compound semiconductor materials. These include GaAs [9], GaP [10–12], ZnS [13], and ZnTe [14] nanowires. Sanatinia et al. think that the second order susceptibility tensor of GaP nanowire comes from both the surface contribution ($\chi_s^{(2)}$) and bulk contribution ($\chi_{bulk}^{(2)}$) [12]. They estimate that $\chi_s^{(2)}$ is larger than $\chi_{bulk}^{(2)}$, and the surface effective thickness is 15–20 nm within the nanowire surface. In our previous study, we observed enhancement of linear EO coefficient in InP nanowires [8]. However, the length of the nanowires showed high variation because of the bottom-up growth approach, which caused uncertainties in determining the filling factor and thus the relationship between the linear EO coefficient and nanowire surface area [15].

In this work, we investigate second order susceptibility in single GaN nanowire with various diameters. The nanowires are fabricated via a top-down approach which ensures that the nanowires

Received 22 July 2020, Accepted 5 September 2020, Scheduled 30 August 2020
* Corresponding author: Haoliang Qian (haoliangqian@zju.edu.cn), Paul K. L. Yu (pyu@ucsd.edu).
[1] Department of Electrical and Computer Engineering, University of California, San Diego, 9500 Gilman Drive, La Jolla, CA 92093, USA. [2] Interdisciplinary Center for Quantum Information, State Key Laboratory of Modern Optical Instrumentation, ZJU-Hangzhou Global Science and Technology Innovation Center, Zhejiang University, Hangzhou 310027, China. [3] Materials Science and Engineering, University of California, San Diego, 9500 Gilman Drive, La Jolla, CA 92093, USA.

are vertical to the substrate with the same height. GaN is selected in our study because not only its wide applications in high speed, high power electronics, and light emitters across the whole visible and infrared wavelengths, but also its different crystal symmetry compared to InP and GaP. In our experiment, the effective second order susceptibility $\chi_{eff}^{(2)}$ at 900 nm is found to be ~ 7 times higher than that of GaN bulk on *c*-sapphire, and our analysis shows that the enhancement of $\chi_{eff}^{(2)}$ mainly comes from the nanowire surface area. The results suggest that the GaN nanowire structures are among the competitive candidates for efficient electro-optic modulator.

A GaN layered structure was grown by metal-organic vapor phase epitaxy (MOVPE) on 2-inch diameter single side polished *c*-plane sapphire wafer using trimethylgallium (TMG) and $NH_{3(g)}$ as precursors for gallium (Ga) and nitrogen (N), respectively. Hydrogen was used as carrier gas, and the total gas flow rate was $\sim$ 5 slm. The GaN layered structure consists of undoped GaN (0.4 µm), GaN buffer layer (0.1 µm). After epitaxy, the wafer was cleaned in standard organic solvents, rinsed in deionized water and blow-dried under nitrogen gas. Single GaN nanowires were patterned by using E-beam lithography (Vistec EBPG 5200). The E-beam nano patterns were then transferred from the HSQ e-beam resist to the GaN layer by dry etching using an Oxford Plasmalab 80 reactive ion etching (RIE) apparatus. The RF power is set at 200 W; Cl_2 at a flow rate of 5 sccm and BCl_3 at 50 sccm were injected. After the dry etching of GaN, buffered oxide etchant (BOE) was used to remove the HSQ from the nanowires. The nanowires have the same height of 432 nm as determined from the RIE etching time. Figure 1 shows a series of single GaN nanowires fabricated.

We performed the reflective SHG measurement of the samples at room temperature in a back-scattering geometry (Figure 2) with mode-locked Ti: Sapphire laser (Mai Tai, Spectra-Physics) operating at 900 nm wavelength at a pulse duration of 100 fs and 80 MHz repetition rate. The laser output power at 900 nm is 2.3 W, and the attenuated incident light power at the GaN nanowire sample

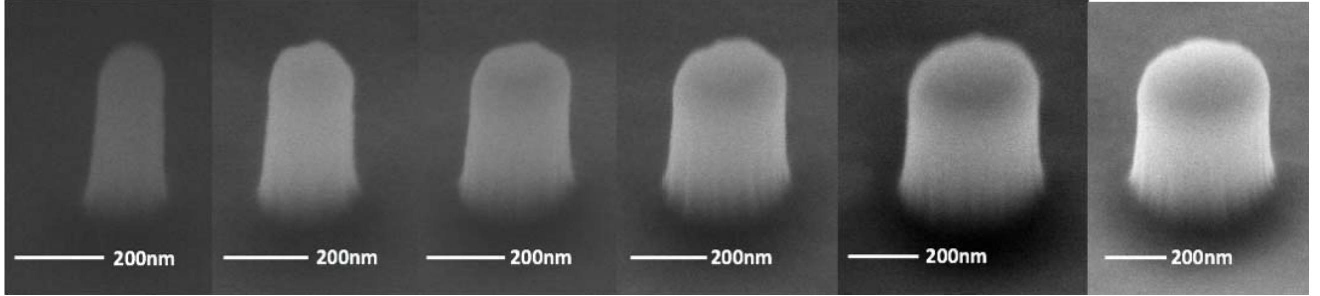

Figure 1. 45° titled SEM images of single nanowires. (diameter (from left to right): 150, 200, 250, 300, 350, and 400 nm).

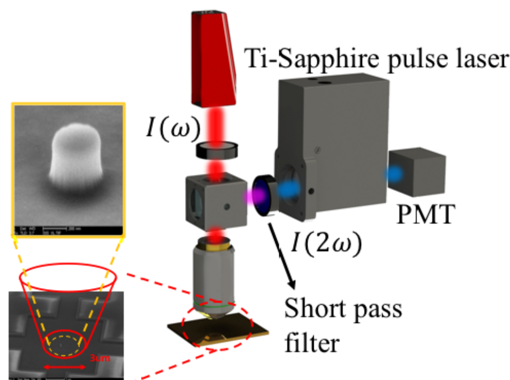

Figure 2. Reflective SHG measurement setup. The single GaN nanowire is at the middle of a focus spot with a 3 µm in diameter spot size.

is 127.6 mW for the focused spot area. A 20X microscope objective lens with a numerical aperture of 0.45 was used. With this configuration, we obtained a laser spot size about 3 µm in diameter.

The reflected fundamental beam and SHG ($\lambda_{2\omega} = 450$ nm) signals were collected by the same objective lens and separated by a dichroic mirror. Several short pass filters (SPF) were used to block the fundamental beam. The SHG signal was directed through a monochromator and subsequently to a photomultiplier tube (PMT). Table 1 lists the intensity of the SHG signals from single GaN nanowires with diameters ranged from 150–400 nm.

Table 1. SHG measurement results for a single GaN nanowire in the range of 150–400 nm diameter (the fundamental excitation is at 900 nm). The transmissivity at 900 nm and the reflectivity at 450 nm are characterized with corresponding incident beam diameter as 3 µm using the same object as for the SHG measurement, which gives the accurate excitation and collection efficiency for the SHG characterization indicating the percentage of the generated SHG being collected by the objective lens. The $\chi^{(2)}_{eff}$ is calculated based on the Equation (3).

Nanowire diameter (nm)		150	200	250	300	350	400
Input Parameters	Input Power (mW)	127.6	127.6	127.6	127.6	127.6	127.6
	Transmissivity (%)	85.2	86.1	85.9	86.6	87.1	85.2
SHG signal	SHG (counts/µs)	80	95	85	245	260	400
	Reflectivity (%)	17.4	14.8	15.2	17.3	17.2	17.4
	$\chi^{(2)}_{eff}$ (pm/V)	136.0	90.2	53.7	58.6	44.2	42.7

2. RESULTS AND DISCUSSION

The SHG measurement techniques have been well documented in the literature. There are three popular methods to measure SHG — phase matched method, parametric fluorescence, and Maker fringe method [16]. The second order nonlinearity is related to the second order susceptibility via

$$P^{(2)}(2\omega) = \epsilon_0 \chi^{(2)} E(\omega)^2 \tag{1}$$

where $P^{(2)}$ is the amplitude of the component of nonlinear polarization oscillation at frequency 2ω, and $\chi^{(2)}$ is the second order susceptibility. For GaN bulk material, most of the reported $\chi^{(2)}$ used the Maker fringe method by rotating a GaN film, with the fundamental beam and SHG generating constructive and destructive interference. The GaN grown on c-sapphire substrate shows a $\chi^{(2)}_{33} \sim 20$ pm/V [17–19]. Its nonlinear effect is originated from the spontaneous polarization and piezoelectricity [20]. In the case of GaN nanowire, due to the lack of a flat film surface, we chose phase matching method to measure its $\chi^{(2)}$. The dangling bonds at the surface lead to a third contribution to the second nonlinear effect. Therefore, the overall effective $\chi^{(2)}$ for GaN nanowires can be expressed as $\chi^{(2)}_{eff} = \chi^{(2)}_{sp} + \chi^{(2)}_{pz} + \chi^{(2)}_{sur}$.

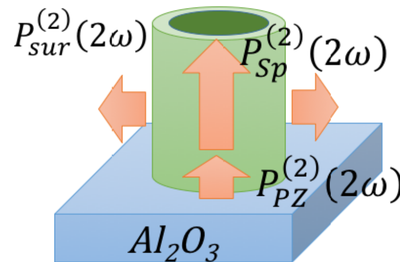

Figure 3. Schematic illustration of the three types of polarizations (spontaneous, piezoelectric, and surface) that contribute SHG from a single GaN nanowire on sapphire (Al_2O_3) substrate.

(sp: spontaneous; pz: piezoelectric; sur: surface) (Figure 3), where $\chi_{sp}^{(2)}$, $\chi_{pz}^{(2)}$ are both intrinsic bulk properties, and $\chi_{sur}^{(2)}$ is the surface contribution. GaN grown on *c*-sapphire substrate has a non-centrosymmetric, hexagonal structure (crystal symmetry: 6 mm) that gives spontaneous polarization in the vertical direction. The lattice mismatch between GaN and sapphire (Al_2O_3) generates piezoelectric polarization [21, 22]. $\chi_{sur}^{(2)}$ is originated from the broken symmetry at the nanowire sidewalls [23], and the surface polarization is not radially distributed, but depends on the broken Ga-N bond.

First, the intensity of the second harmonic signals, $I(2\omega)$, is related to the amplitudes as

$$I(2\omega) \propto \left[P^{(2)}(2\omega)\right]^2 \propto \left[P_{sur}^{(2)}(2\omega)\right]^2 + \left[P_{bulk}^{(2)}(2\omega)\right]^2 \propto \left[\chi_{sur}^{(2)} E^2(\omega)\right]^2 + \left[\chi_{bulk}^{(2)} E^2(\omega)\right]^2$$
$$\propto \left[(\chi_{sur}^{\prime(2)} \cdot r \cdot S) \cdot E^2(\omega)\right]^2 + \left[(\chi_{bulk}^{\prime(2)} \cdot V) \cdot E^2(\omega)\right]^2 \propto A_{sur} \cdot S^2 + B_{bulk} \cdot V^2. \quad (2)$$

Herein, we define $P_{sur}^{(2)}(2\omega)$ and $P_{bulk}^{(2)}(2\omega)$ as the amplitude of the component of nonlinear polarization at the surface and in the bulk at frequency 2ω, respectively. $\chi_{sur}^{\prime(2)}$ and $\chi_{bulk}^{\prime(2)}$ are the surface and volume distributed second harmonic susceptibility, respectively. r represents the surface effective thickness along the radius direction [12]. A_{sur} is the coefficient related to the nanowire surface contribution, and B_{bulk} is the coefficient related to the bulk contribution. S is the nanowire's surface area, and V is the nanowire's volume. In Table 2, the fitting results show that the SHG from single GaN nanowire is more dominated by the surface effect. Figure 4(a) shows the measured SHG signal counts and the fitting results based on Equation (2). Figure 4(b) is the normalized SHG counts versus different diameters of single nanowire, one can see the increasing percentage of the surface contribution to SHG as the diameter of the nanowire decreases. We also observed that when GaN nanowire diameter is in the range of 150–400 nm, the volume of the nanowire only accounts for $< 10\%$ of the SHG signals.

Table 2. The SHG fitting result for different diameters of the GaN nanowire. The SHG is received by subtracting the SHG from the single GaN nanowire to the background noise. The SHG counts here are considered with the collection efficiency compared with the numbers in Table 1. Two variables linear regression fitting was applied to receive $A_{sur} \cdot S^2$ and $B_{bulk} \cdot V^2$.

Nanowire diameter (nm)	**$S^2 \times 10^{26}$ (m^4)**	**$V^2 \times 10^{40}$ (m^6)**	**SHG (counts/μs)**	**$A_{sur} \cdot S^2$**	**$B_{bulk} \cdot V^2$**
150	4.2	0.6	460	287.8	3.9
200	7.4	1.9	643	512.0	12.4
250	12	4.5	558	795.7	30.2
300	17	9.3	1420	1148.6	62.5
350	23	17	1509	1563.8	116.3
400	30	30	2304	2041.2	198.3

Second, the second harmonic susceptibility, $\chi^{(2)}$, of single GaN nanowire is an important factor to evaluate its potential use in electrooptic modulator. To measure $\chi_{eff}^{(2)}$ of single GaN nanowires ($\chi_{eff}^{(2)} = \chi_{sp}^{(2)} + \chi_{pz}^{(2)} + \chi_{sur}^{(2)}$), we accurately characterize the system setup, including: 1. actual power excites the single nanowire (input power in Table 1); 2. objective lens collection efficiency for the SHG signal (SHG reflectivity in Table 1); 3. The detection efficiency includes the monochromator and the photomultiplier tube (4.87%). The relationship between the SHG intensity and second harmonic susceptibility can be written as [2]

$$I(2\omega, l) = \frac{\omega^2 (\chi_{eff}^{(2)})^2 l^2}{2 n_{2\omega} n_\omega^2 c^3 \epsilon_0} \left(\frac{\sin(\Delta k l/2)}{\Delta k l/2}\right)^2 I^2(\omega). \quad (3)$$

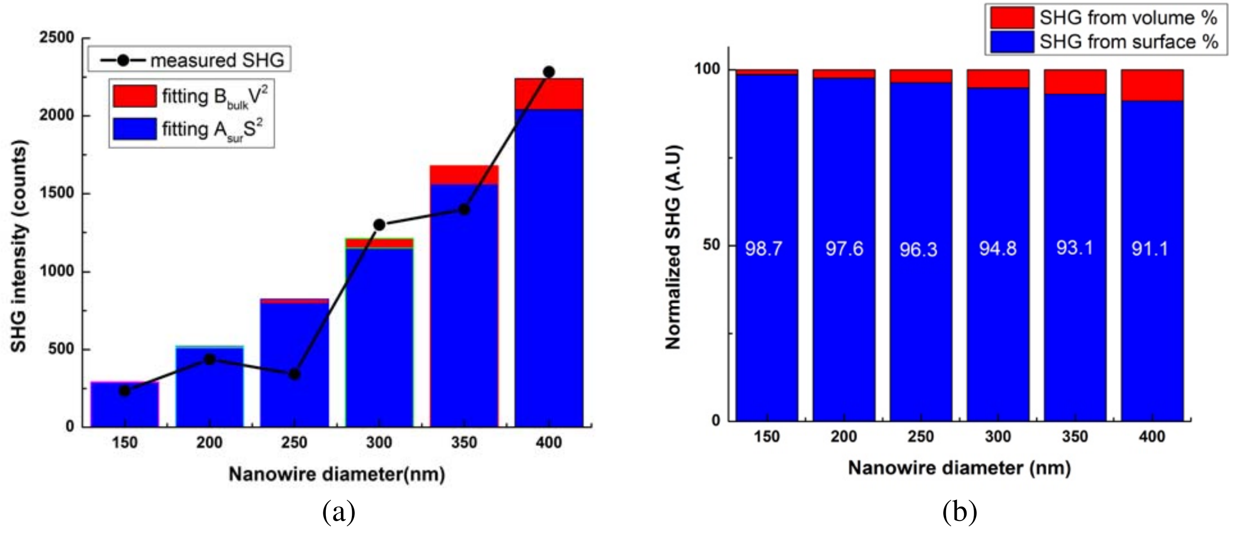

Figure 4. (a) The measured SHG and fitting result based on Equation (2). (b) The percentage of SHG generated from the surface (blue) and the bulk (red) are displayed with the surface percentage shown.

$I(2\omega, l)$ is the intensity of SHG for nanowire with length l, $I(\omega)$ the intensity of fundamental light, ω the light frequency, $\chi^{(2)}_{\mathit{eff}}$ the effective second harmonic susceptibility, and $n_{2\omega}$ and n_ω are the refractive indices of light at frequencies ω and 2ω, respectively [24]. $\sin(\Delta kl/2)/\Delta kl/2$ is the phase matching term, c the light speed, and ϵ_o the vacuum permittivity. Since nanowires are only 432 nm in height, and the majority of the nonlinear contribution comes from the surface area, the phase-matched term can be eliminated. Note that $\chi^{(2)}_{\mathit{eff}}$ is normalized to the fill factor (FF). From the SHG measurement results shown in Table 1, as the diameter of the nanowire decreases, the $\chi^{(2)}_{\mathit{eff}}$ is seen to increase. For 150 nm diameter nanowire, $\chi^{(2)}_{\mathit{eff}}$ reaches 136 pm/V, which is ~ 7 times higher than GaN bulk ($\chi^{(2)}_{33} =\sim 20$ pm/V). The narrower the nanowire is, the higher the surface-to-volume ratio is. Consequently, the $\chi^{(2)}_{\mathit{eff}}$ of narrower nanowires is influenced more by the surface term ($\chi^{(2)}_{sur}$).

Our results and analysis show that the surface polarization is dominant when GaN nanowire diameter goes down below 400 nm. Since the surface polarization is larger than the bulk polarization (summation of the spontaneous and piezoelectric polarizations), when the nanowire diameter is reduced, the surface-to-volume ratio increases, and the $\chi^{(2)}_{\mathit{eff}}$ increases as well. Based on our results, we project if the diameter of nanowire is below 50 nm, its effective $\chi^{(2)}$ will exceed that of $LiNbO_3$. Also, the SHG enhancement contributed from nanowire surface area can be applied to other nano-material structures. The large $\chi^{(2)}_{\mathit{eff}}$ obtained from the GaN nanowires makes the high-speed and efficient electro-optic modulators on GaN platform one step closer to the reality.

ACKNOWLEDGMENT

This work is supported by the ONR-Multidisciplinary University Research Initiative (MURI) (grant number: N00014-13-1-0678). We acknowledge Dr. Maria Isabel Montero Ramirez for electron beam lithography writing and Dr. Dingbo Chen for the nanowire fabrication suggestion.

REFERENCES

1. Pantazis, P., J. Maloney, D. Wu, and S. E. Fraser, "Second harmonic generating (SHG) nanoprobes for in vivo imaging," *Proceedings of the National Academy of Sciences*, Vol. 107, 14535–14540, 2010.

2. Boyd, R. W., *Nonlinear Optics*, 3rd Edition, Academic Press, Orlando, FL, USA, 2008.
3. Wooten, E. L., et al., "A review of lithium niobate modulators for fiber-optic communications systems," *IEEE J. Sel. Top. Quantum Electron.*, Vol. 6, 69–82, 2000.
4. Jacobsen, R. S., et al., "Strained silicon as a new electro-optic material," *Nature*, Vol. 441, 199–202, 2006.
5. Puckett, M. W., et al., "Tensor of the second-order nonlinear susceptibility in asymmetrically strained silicon waveguides: Analysis and experimental validation," *Opt. Lett.*, Vol. 39, 1693–1696, 2014.
6. Shi, Y., et al., "Low (sub-1-volt) halfwave voltage polymeric electro-optic modulators achieved by controlling chromophore shape," *Science*, Vol. 288, 119–122, 2000.
7. Alloatti, L., et al., "Second-order nonlinear optical metamaterials: ABC-type nanolaminates," *Appl. Phys. Lett.*, Vol. 107, 121903, 2015.
8. Novotny, C. J., C. T. DeRose, R. A. Norwood, and P. K. L. Yu, "Linear electrooptic coefficient of InP nanowires," *Nano Lett.*, Vol. 8, 1020–1025, 2008.
9. Bautista, G., et al., "Second-harmonic generation imaging of semiconductor nanowires with focused vector beams," *Nano Lett.*, Vol. 15, 1564–1569, 2015.
10. Sanatinia, R., M. Swillo, and S. Anand, "Surface second-harmonic generation from vertical GaP nanopillars," *Nano Lett.*, Vol. 12, 820–826, 2012.
11. Sanatinia, R., S. Anand, and M. Swillo, "Experimental quantification of surface optical nonlinearity in GaP nanopillar waveguides," *Opt. Express*, Vol. 23, 756–764, 2015.
12. Sanatinia, R., S. Anand, and M. Swillo, "Modal engineering of second-harmonic generation in single GaP nanopillars," *Nano Lett.*, Vol. 14, 5376–5381, 2014.
13. Hu, H., et al., "Precise determination of the crystallographic orientations in single ZnS nanowires by second-harmonic generation microscopy," *Nano Lett.*, Vol. 15, 3351–3357, 2015.
14. Liu, W., et al., "Laterally emitted surface second harmonic generation in a single ZnTe nanowire," *Nano Lett.*, Vol. 13, 4224–4229, 2013.
15. Novotny, C. J. and P. K. L. Yu, "Vertically aligned, catalyst-free InP nanowires grown by metalorganic chemical vapor deposition," *Appl. Phys. Lett.*, Vol. 87, 203111, 2005.
16. Sutherland, R. L., *Handbook of Nonlinear Optics*, CRC Press, 2003.
17. Long, X. C., et al., "GaN linear electro-optic effect," *Appl. Phys. Lett.*, Vol. 67, 1349–1351, 1995.
18. Miragliotta, J., D. Wickenden, T. Kistenmacher, and W. Bryden, "Linear-and nonlinear-optical properties of GaN thin films," *JOSA B*, Vol. 10, 1447–1456, 1993.
19. Xiong, C., et al., "Integrated GaN photonic circuits on silicon (100) for second harmonic generation," *Opt. Express*, Vol. 19, 10462–10470, 2011.
20. Abe, M., et al., "Accurate measurement of quadratic nonlinear-optical coefficients of gallium nitride," *J. Opt. Soc. Am. B*, Vol. 27, 2026–2034, 2010.
21. Yu, E. T., et al., "Spontaneous and piezoelectric polarization effects in III–V nitride heterostructures," *Journal of Vacuum Science & Technology B: Microelectronics and Nanometer Structures Processing, Measurement, and Phenomena*, Vol. 17, 1742–1749, 1999.
22. Bernardini, F., V. Fiorentini, and D. Vanderbilt, "Spontaneous polarization and piezoelectric constants of III-V nitrides," *Phys. Rev. B*, Vol. 56, R10024–R10027, 1997.
23. Shen, Y. R., "Surface properties probed by second-harmonic and sum-frequency generation," *Nature*, Vol. 337, 519–525, 1989.
24. Barker, A. S. and M. Ilegems, "Infrared lattice vibrations and free-electron dispersion in GaN," *Phys. Rev. B*, Vol. 7, 743–750, 1973.